A Pseudodynamic Testing Algorithm for Obtaining Seismic Responses of Structures

Shuenn-Yih Chang[1], Chiu-Li Huang[2]

[1]*National Taipei University of Technology, E-mail: changsy@ntut.edu.tw*

[2]*Fu Jen Catholic University, E-mail: 003951@mail.fju.edu.tw*

ABSTRACT

A novel family method is proposed for the pseudodynamic tests. It can integrate favourable numerical properties together, such as the unconditional stability, explicit formulation, second-order accuracy and favourable numerical dissipation. Since this family method can have an explicit formulation of each time step its pseudodynamic implementation involves no iteration procedure. Consequently, the pseudodynamic tests can be easily conducted when compared to an implicit pseudodynamic method, where an iteration procedure must be involved for each time step. On the other hand, the properties of unconditional stability, second order accuracy and numerical dissipation indicate that the proposed pseudodynamic algorithm is very promising for solving inertial problems, where the total response is dominated by low frequency modes only and the high frequency responses are of no interest. The unconditional stability implies that there is no limitation on step size for the high frequency modes. Besides, the dominated low frequency modes can be reliably integrated by choosing an appropriate time step since the proposed family method can have a second order accuracy. Finally, the spurious participation of high frequency responses can be suppressed or filtered out by the desired numerical dissipation. The proposed pseudodynamic algorithm is very promising for a general pseudodynamic test or a substructure pseudodynamic test.

Keywords: *pseudodynamic test, numerical dissipation, structure-dependent method, unconditional stability*

1 INTRODUCTION

In a pseudodynamic test, an integration algorithm is applied to solve the equations of motion and it is performed both experimentally and numerically [1]. In general, both the inertial forces and the damping forces of the specimen are analytically modelled, and the restoring forces are experimentally measured from the specimen. For each step, the command displacements of the specimen are first computed and are imposed upon the specimen by servo-hydraulic actuators. Once the command displacements are achieved, their corresponding restored forces are experimentally measured and are used to determine the next command displacements for the subsequent time step. This procedure can be repeated until the desired response time history is obtained. The pseudo-dynamic test is different from the quasi-static or cyclic loading tests due to the feedback procedure. In general, errors introduced in any time step will be propagated and accumulated through the feedback procedure [2–5]. Hence, pseudodynamic errors must be controlled within certain limits so that reliable test results can be achieved.

Many integration methods have been used to conduct pseudodynamic tests. However, the explicit pseudodynamic algorithms [6–7] are preferred over the implicit pseudodynamic algorithms [8–10] since they involve no nonlinear iterations and thus their implementation are simple when

[1] Professor, changsy@ntut.edu.tw

[2] Instructor, 003951@mail.fju.edu.tw

* Corresponding author

compared to implicit pseudodynamic algorithms. However, only a few explicit algorithms [11–15] are available, such as the Newmark explicit method [11]. Meanwhile, two families of dissipative explicit algorithms have been proposed by Chang [12]. However, they are only conditionally stable. To overcome conditional stability, implicit pseudodynamic algorithms have been implemented. However, their implementations become more complex and need some extra hardware [8–10] when compared to the explicit pseudodynamic algorithms. The HHT$-\alpha$ method [16] is a widely used implicit algorithm for structural dynamics since it has unconditional stability; and favourable numerical dissipation to filter out the spurious growth of high frequency modes, which might arise from numerical and experimental errors during the tests. However, it requires an iteration procedure within each time step in the solution of a nonlinear system. In performing a pseudodynamic test, nonlinear iterations might lead to incorrect loading and unloading hysteretic loops in the specimen and thus result in an inaccurate or even an unstable test result. Hence, some different techniques have been proposed to overcome the difficulty caused by nonlinear iterations for using HHT$-\alpha$ method [8-10].

It is well recognized that an explicit algorithm can only have conditional stability while an iteration procedure is needed for an implicit algorithm although both the explicit and implicit algorithms can have desired numerical dissipation. Chang explicit method is the first structure-dependent integration method to integrate the unconditional stability and explicit formulation together [12]. Although some similar structure-dependent integration methods with improved properties have been developed they possess no favourable numerical dissipation. In order to introduce numerical dissipation into an unconditionally stable, explicit algorithm, a novel family of explicit method is proposed. Numerical properties of this family of pseudodynamic algorithms are investigated and numerical simulations are applied to confirm the analytical predictions. Finally, actual pseudodynamic tests were conducted to confirm the feasibility of this family method.

2 PROPOSED ALGORITHM

For a multiple degree of freedom system, the proposed family method (PFM) can be expressed as:

$$\begin{aligned}
&\mathbf{M}\mathbf{a}_{i+1}+\mathbf{C}_0\mathbf{v}_{i+1}+(1+\alpha)\mathbf{K}\mathbf{d}_{i+1}-\alpha\mathbf{K}\mathbf{d}_i=(1+\alpha)\mathbf{f}_{i+1}-\alpha\mathbf{f}_i\\
&\mathbf{d}_{i+1}=\mathbf{B}_0\mathbf{d}_{i-1}+\mathbf{B}_1\mathbf{d}_i+\mathbf{B}_2(\Delta t)\mathbf{v}_i+\mathbf{B}_3(\Delta t)^2\mathbf{a}_i \qquad .\\
&\mathbf{v}_{i+1}=\mathbf{v}_i+(\Delta t)\left[(1-\gamma)\mathbf{a}_i+\gamma\mathbf{a}_{i+1}\right]
\end{aligned} \tag{1}$$

where $\mathbf{M}$, $\mathbf{C}_0$ and $\mathbf{K}$ are mass, viscous damping and stiffness matrices; $\mathbf{d}_i$, $\mathbf{v}_i$, $\mathbf{a}_i$ and $\mathbf{f}_i$ are nodal vectors of displacement, velocity, acceleration and external force at the end of the $i-th$ time step, respectively, and the coefficient matrices of $\mathbf{B}_0$ to $\mathbf{B}_3$ are expressed as:

$$\begin{aligned}
\mathbf{B}_0&=-\alpha\beta\sigma\left[\mathbf{M}+\gamma(\Delta t)\mathbf{C}_0+(1+\alpha)\beta\sigma(\Delta t)^2\mathbf{K}_0\right]^{-1}(\Delta t)^2\mathbf{K}_0\\
\mathbf{B}_1&=\mathbf{I}+\alpha\beta\sigma\left[\mathbf{M}+\gamma(\Delta t)\mathbf{C}_0+(1+\alpha)\beta\sigma(\Delta t)^2\mathbf{K}_0\right]^{-1}(\Delta t)^2\mathbf{K}_0\\
\mathbf{B}_2&=\left[\mathbf{M}+\gamma(\Delta t)\mathbf{C}_0+(1+\alpha)\beta\sigma(\Delta t)^2\mathbf{K}_0\right]^{-1}\left[\mathbf{M}+\gamma(\Delta t)\mathbf{C}_0\right]\\
\mathbf{B}_3&=\left[\mathbf{M}+\gamma(\Delta t)\mathbf{C}_0+(1+\alpha)\beta\sigma(\Delta t)^2\mathbf{K}_0\right]^{-1}\left[\tfrac{1}{2}\mathbf{M}-(\beta-\tfrac{1}{2}\gamma)(\Delta t)\mathbf{C}_0\right]
\end{aligned} \qquad . \tag{2}$$

where $\mathbf{K}_0$ is the initial stiffness matrix and the current stiffness matrix $\mathbf{K}$ in the first line of Eq.(1) is generally different from $\mathbf{K}_0$ for a nonlinear system. In addition, $\mathbf{C}_0$ is an initial damping matrix and is often determined from the initial structural properties. In a pseudodynamic test, the restoring force vectors $\mathbf{r}_i$ is often applied to replace $\mathbf{K}\mathbf{d}_i$ in the first line of Eq. (1). The parameters of α, β,

γ and σ are used to govern the numerical properties. In general, the following relations are recommended:

$$-\frac{1}{3} \le \alpha \le 0 \quad , \quad \beta = \frac{(1-\alpha)^2}{4} \quad \text{and} \quad \gamma = \frac{1}{2} - \alpha \, . \tag{3}$$

so that PFM can have unconditional stability, second-order accuracy and favorable numerical dissipation for $\sigma \ge 1$. The parameter σ is a stability amplification factor, which has been proposed by Chang [17] to enlarge the unconditional stability range for a structure-dependent integration method, and $\sigma = 2$ is highly recommended for practical applications.

3 NUMERICAL PROPERTIES

To gain inside into the numerical properties of PFM for a nonlinear system, a parameter δ_i is introduced to monitor the stiffness change. It is defined as the ratio of the stiffness at the end of the $i-th$ time step k_i over the initial stiffness k_0, i.e., $\delta_i = k_i / k_0$; δ_i is the instantaneous degree of nonlinearity at the end of the $i-th$ time step. As a result, $\delta_i = 1$ means the instantaneous stiffness equal to the initial stiffness. Whereas, $\delta_i > 1$ implies that the instantaneous stiffness is greater than the initial stiffness; $\delta_i < 1$ implies that the instantaneous stiffness is less than the initial stiffness. The analysis of an integration method can be found in the references [14, 17] and will not be elaborated herein.

3.1 A Stability Amplification Factor

To examine the performance of σ, the variation of the upper stability limit with δ_i for the subfamily of PFM defined in Eq. (3) is plotted in Fig. 1a for $\alpha = 0$, which implies $\beta = 1/4$ and $\gamma = 1/2$. The curve is invisible in the unconditional stability range since in this range its upper stability limit is infinitely large. The unconditional stability range is extended from $\delta_i \le 1 - \xi^2$ to $\delta_i \le \sigma - \xi^2$ if $\sigma > 1$ is applied to the method.

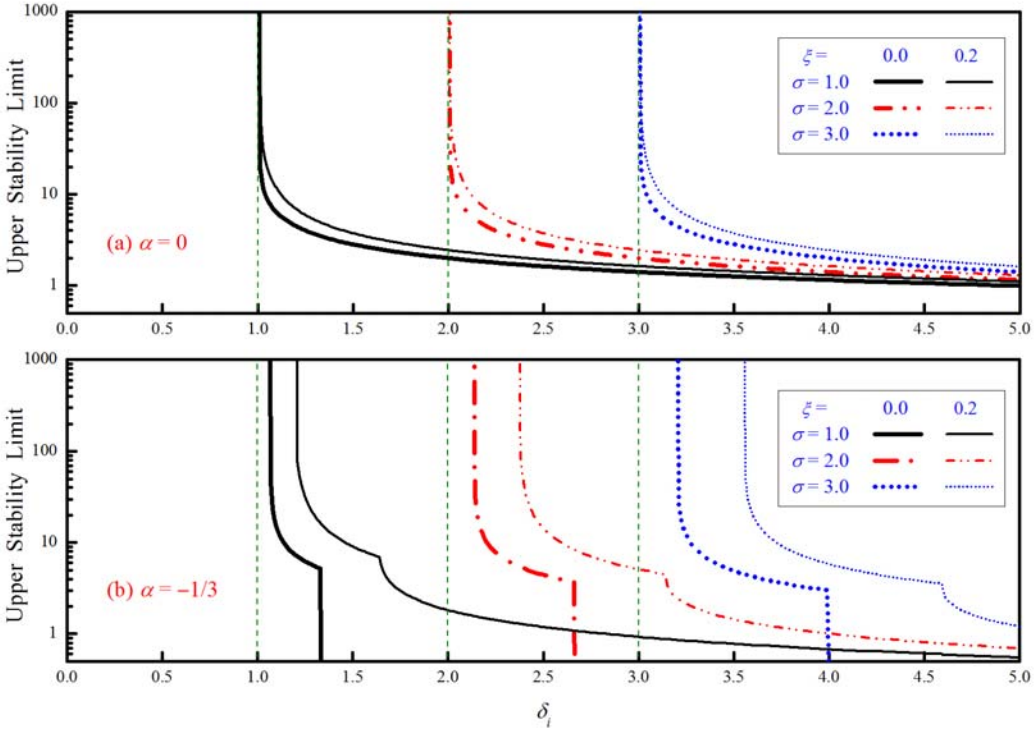

Figure 1 - Variation of upper stability limit with δ_i for proposed family method

It is also of interest to consider the case of $\alpha \neq 0$ for the subfamily defined in Eq. (3). In fact, the case of $\alpha = -1/3$ is considered and the results are shown in Fig. 1b. Comparing Fig. 1a to 1b, the algorithm with $\alpha = -1/3$ has a larger unconditional stability range in each corresponding curve when compared to that of $\alpha = 0$. In addition, there is a point, which has an abrupt change of slope, in each curve. At this point, the two real principal roots bifurcate into complex conjugate roots. It is verified that the stability amplification factor σ can enlarge the unconditional stability range and a large σ results in a large unconditional stability range. However, it is very rare to experience that for a real structure the instantaneous stiffness is as large as twice of the initial stiffness, i.e., $\delta_i > 2$. Hence, $\sigma = 2$ is highly recommended for practical applications.

3.2 Stability

The spectral radius is defined as $\rho(\mathbf{A}_i) = \max|\lambda_k|$ for $k = 1$, 2 and 3, where λ_k is an eigenvalue of the amplification $\mathbf{A}_i$. For PFM with $\xi = 0$, the variation of spectral radius with $\Delta t / T_0$ are shown in Fig. 2 for different instantaneous degree of nonlinearity and different α values. Many combinations of δ_i and δ_{i+1} can be used to simulate a variety of nonlinear cases. However, only the cases of $\delta_i = \delta_{i+1} = 0.5$, 1.0 and 2.0 are considered in this paper since δ_i is generally very close to δ_{i+1} for the two consecutive time steps in a step-by-step integration procedure.

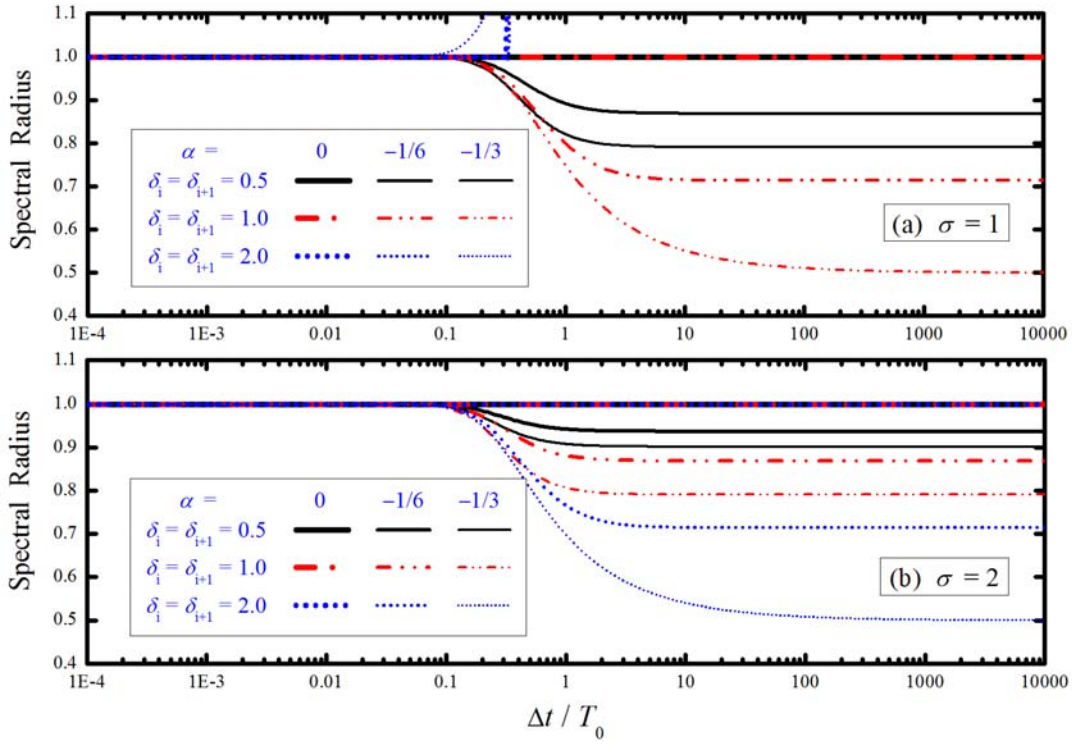

Figure 2 - Variation of spectral radius with $\Delta t / T_0$ for proposed family method

In Fig. 2a, the spectral radius is generally less than or equal to 1 as $\delta_i = \delta_{i+1} \leq 1$ and finally tends to a certain constant. Whereas, it becomes to be greater than 1 after a certain value of $\Delta t / T_0$ as $\delta_i = \delta_{i+1} > 1$. Meanwhile, the spectral radius is less than or equal to 1 as $\delta_i = \delta_{i+1} \leq 2$ in Fig. 2b. This phenomenon is consistent with the previous study of the stability amplification factor σ. Thus, these results attest to that the application of σ to the algorithms can enlarge the unconditional stability range from $\delta_i \leq 1$ to $\delta_i \leq \sigma$. In general, each curve has a unit spectral radius for small $\Delta t / T_0$ while it decreases step by step and finally tends to a certain constant. For given $\delta_i = \delta_{i+1}$ and $\Delta t / T_0$, the spectral radius decreases with the decrease of α. Whereas, for given α and $\Delta t / T_0$, it decreases

with the increase of $\delta_i = \delta_{i+1}$. Notice that $T_0 = 2\pi / \omega_0$ and $\omega_0 = \sqrt{k_0 / m}$ is the initial natural frequency of the system.

3.3 Accuracy

A bounded oscillatory response can be obtained if the two principal eigenvalues of the amplification matrix $\mathbf{A}_{i+1}$ are complex conjugates. Figure 3 shows the variation of relative period error with $\Delta t / T_0$ for different combinations of α and δ_i for both $\sigma = 1$ and 2.

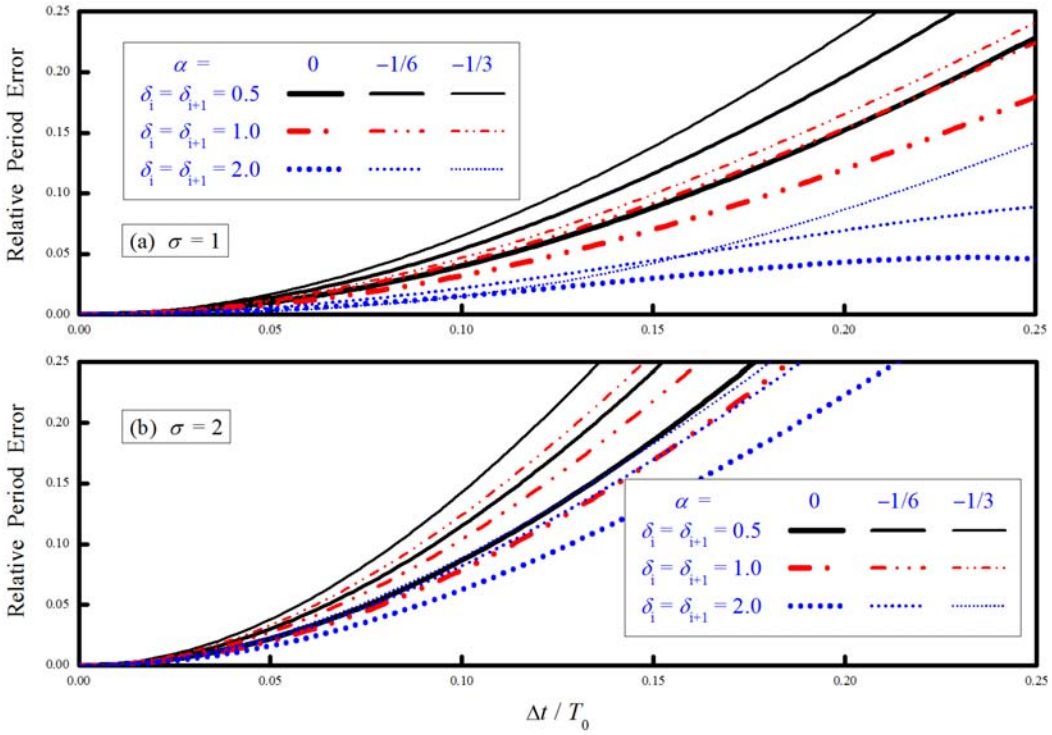

Figure 3 - Variation of relative period error with $\Delta t / T_0$ for proposed family method

The relative period error increases with increasing $\Delta t / T_0$ as δ_i and α are given. Period elongation is found for PFM and its amount increases with the decrease of α for a given δ_i while it decreases with the increase of δ_i for a given value of α. After comparing the corresponding curves in Fig. 3a to those in Fig. 3b, the relative period error for the case of $\sigma = 2$ is slightly larger than that of the case of $\sigma = 1$ for a small $\Delta t / T_0$. In fact, the increase of σ leads to the increase of period distortion. This will somewhat limit the choice of a large σ value although it will enlarge the unconditional stability range from $\delta_i \le 1$ to $\delta_i \le \sigma$. It is seen in Fig. 3 that the relative period error is insignificant for a small $\Delta t / T_0$, such as $\Delta t / T_0 \le 0.05$. This implies that PFM can give a reliable solution for a nonlinear system if a time step is chosen to meet $\Delta t / T_0 \le 0.05$ for the modes of interest.

3.4 Numerical Damping Ratio

The variation of numerical damping ratio with $\Delta t / T_0$ for PFM can be obtained from the two complex conjugate eigenvalues of the amplification matrix. Figure 4 reveals that there is no numerical dissipation for the case of $\alpha = 0$ for both $\sigma = 1$ and 2. Whereas, the numerical damping ratio increases with $\Delta t / T_0$ for PFM with $\alpha = -1/6$ and $-1/3$ as $\delta_i \le 1$. In addition, it also increases with the decrease of α for a given $\Delta t / T_0$ as $\delta_i \le 1$. However, very different phenomena are found

between $\sigma = 1$ and 2 for the case of $\delta_i = \delta_{i+1} = 2$. In Fig. 4a, the three curves for $\alpha = 0$, $-1/6$ and $-1/3$ stop at the bifurcation points where the complex conjugate roots become real roots. On the other hand, in Fig. 4b, the curve for $\alpha = 0$ leads to zero numerical damping, and the curves for $\alpha = -1/6$ and $-1/3$ can result in favourable numerical dissipation. As a summary, favourable numerical dissipation can be generally obtained from PFM with an appropriate value of $\sigma \geq 1$ and the choice of $-1/3 \leq \alpha < 0$ if $\delta_i \leq \sigma$ is satisfied during the step-by-step integration procedure.

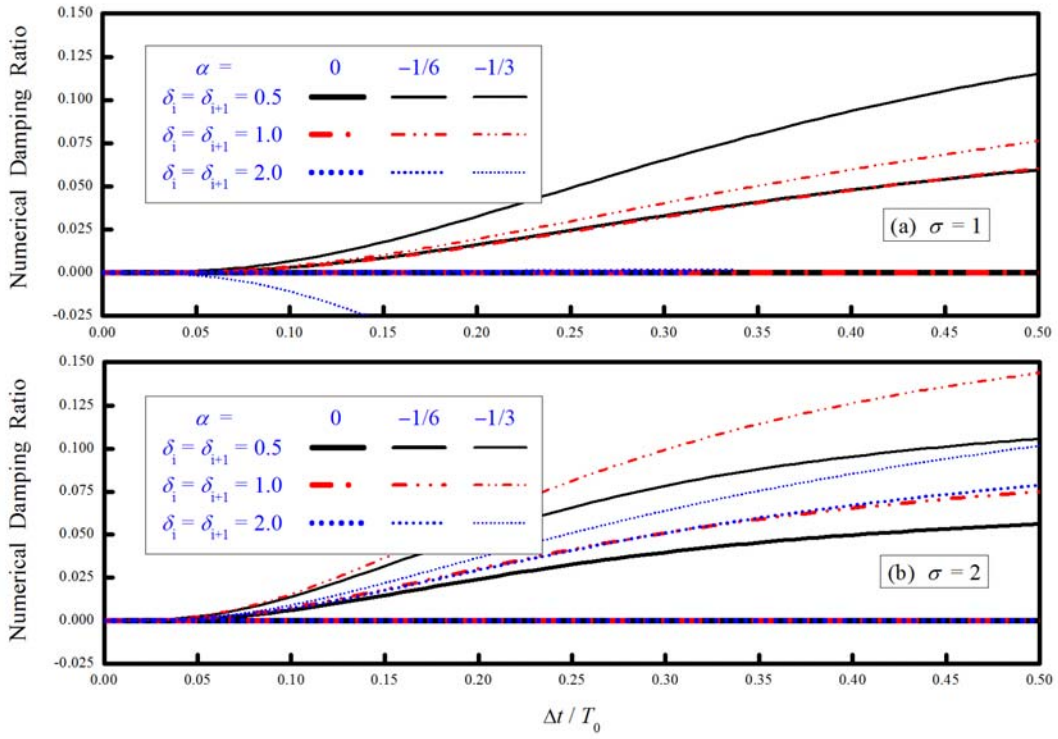

Figure 4 - Variation of numerical damping ratio with $\Delta t / T_0$ for proposed family method

4 IMPLEMENTATION

It is apparent that PFM is very promising for the pseudodynamic testing, especially for a substructure pseudodynamic test since it has the unconditional stability, explicitness of each time step and favourable numerical dissipation. Therefore, it is of great interest to examine its actual performance in conducting a pseudodynamic test. For this purpose, its implementation for a pseudodynamic test is sketched next for the subsequent applications.

In general, the restoring force vector $\mathbf{r}_i$ is often used to replace $\mathbf{K}\mathbf{d}_i$ in the first line of Eq. (1) in the nonlinear dynamic analysis or the pseudodynamic testing. Before conducting a pseudo-dynamic test, it is necessary to determine the initial viscous damping matrix $\mathbf{C}_0$ and initial stiffness matrix $\mathbf{K}_0$ to yield the denominator $\mathbf{M} + \gamma(\Delta t)\mathbf{C}_0 + (1+\alpha)\beta\sigma(\Delta t)\mathbf{K}_0$ for the coefficients of $\mathbf{B}_0$ to $\mathbf{B}_3$, and thus the final form of the coefficient matrices of $\mathbf{B}_0$ to $\mathbf{B}_3$. Next, the displacement vector $\mathbf{d}_{i+1}$ for the next time step can be directly calculated from the use of the second line of Eq. (1) and is numerically equivalent to solve:

$$\begin{aligned}&\left[\mathbf{M} + \gamma(\Delta t)\mathbf{C}_0 + (1+\alpha)\beta(\Delta t)^2\mathbf{K}_0\right]\mathbf{d}_{i+1} = \alpha\beta(\Delta t)^2\mathbf{K}_0(\mathbf{d}_i - \mathbf{d}_{i-1}) \\ &+\left[\mathbf{M} + (1+\alpha)\beta(\Delta t)^2\mathbf{K}_0\right]\mathbf{d}_i + \left[\mathbf{M} + \gamma(\Delta t)\mathbf{C}_0\right](\Delta t)\mathbf{v}_i + \left[\tfrac{1}{2}\mathbf{M} - (\beta - \tfrac{1}{2}\gamma)(\Delta t)\mathbf{C}_0\right](\Delta t)^2\mathbf{a}_i\end{aligned} \quad . \tag{4}$$

After obtaining $\mathbf{d}_{i+1}$, servo hydraulic actuators are used to impose these computed displacements upon the specimen. The corresponding restoring force $\mathbf{r}_{i+1}$ developed by the specimen can be measured. The term $\mathbf{a}_{i+1}$ can be expressed in terms of $\mathbf{r}_{i+1}$ and $\mathbf{v}_{i+1}$ by using the first line of Eq. (1).

Next, $\mathbf{v}_{i+1}$ can be obtained after substituting this result into the third line of Eq. (1) and has the following formulation:

$$\left[\mathbf{M}+\gamma(\Delta t)\mathbf{C}_0\right]\mathbf{v}_{i+1}=\left\{\mathbf{M}\left[\mathbf{v}_i+(1-\gamma)(\Delta t)\mathbf{a}_i\right]+\gamma(\Delta t)\left[(1+\alpha)\mathbf{f}_{i+1}-\alpha\mathbf{f}_i-(1+\alpha)\mathbf{r}_{i+1}+\alpha\mathbf{r}_i\right]\right\}. \quad (5)$$

Finally, $\mathbf{a}_{i+1}$ can be calculated by using the equation of motion. This test procedure can be repeated until the desired time history is achieved. It is very important to note that this test procedure is exactly the same as that for the widely used Newmark explicit method.

In general, a Gaussian elimination method can be applied to solve Eq. (4) and (5), and it consists of a triangulation and a substitution for each time step. It is important to note that either the matrix of $\mathbf{M}+\gamma(\Delta t)\mathbf{C}_0+(1+\alpha)\beta\sigma(\Delta t)^2\mathbf{K}_0$ or $\mathbf{M}+\gamma(\Delta t)\mathbf{C}_0$ is needed to be triangulated only once since it is invariant for a whole integration procedure. In an elimination method, a triangulation consumes much more computational efforts than a substitution. Since the triangulation is performed only once in the solution of a nonlinear system for a whole integration procedure, PFM will involve commensurate computational efforts for each time step when compared to an explicit method, such as the Newmark explicit method.

5 PSEUDODYNAMIC TESTS

In order to confirm the feasibility of PFM, a series of pseudodynamic tests were conducted for 2-degree-of-freedom systems. Each test specimen has a relatively high second mode when compared to the first mode. The higher mode will lead to more severe error propagation and thus the merit of using numerical damping to suppress error propagation can be confirmed. Several steel beams with the cross section of $\mathrm{H}\,100\times100\times6\times8$ and a length of $2.2\ m$ were adopted for the serial tests. The experimental test setup is plotted in Fig. 5.

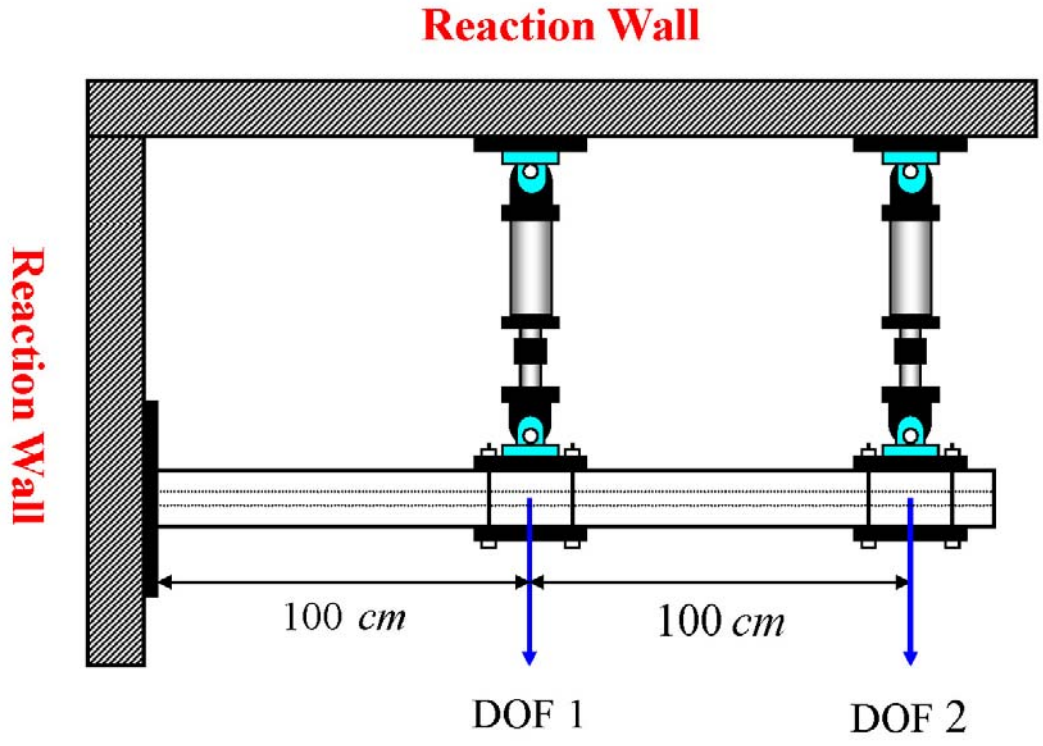

Figure 5 - Pseudodynamic test setup for 2-degree-of-freedom system

5.1 Free Vibration Response

Two members of PFM were selected to perform the pseudodynamic tests. For brevity, the use of PFM with $\alpha=0$ and $\sigma=2$ is referred as PFM1 while that with $\alpha=-1/3$ and $\sigma=2$ is referred as

PFM2. Before performing a pseudodynamic test, the mass matrix should be specified first. In addition, the initial stiffness matrix must be experimentally measured to determine the coefficient matrices. As a result, they are found to be:

$$\mathbf{M} = \begin{bmatrix} 5.0\times10^{4} & 0 \\ 0 & 5.0\times10^{3} \end{bmatrix} kg \qquad \mathbf{K}_0 = \begin{bmatrix} 9.30\times10^{5} & -1.91\times10^{6} \\ -1.91\times10^{6} & 4.55\times10^{6} \end{bmatrix} N/m. \tag{6}$$

Based on these initial structural properties, the initial natural frequencies of this system are found to be 1.59 and 30.43 rad/sec. In addition, their corresponding modal shapes, ϕ_1 and ϕ_2, are found to be:

$$\phi_1 = \begin{Bmatrix} 1.000 \\ 0.421 \end{Bmatrix} \qquad \phi_2 = \begin{Bmatrix} -0.042 \\ 1.000 \end{Bmatrix}. \tag{7}$$

Two different initial displacement vectors with zero velocity are considered. One contains the pure first mode and the other consists of both two modes i.e., $\mathbf{d}_0^{(p)} = 15\phi_1$ and $\mathbf{d}_0^{(c)} = 15\phi_1 + 7.5\phi_2$ mm. The results to these two different initial conditions are plotted in Fig. 6. The response to the initial displacement $\mathbf{d}_0^{(p)}$ is obtained from the Newmark explicit method (NEM) with $\Delta t = 0.01$ sec, which can be considered as a reference solution for comparison. Whereas, those responses to $\mathbf{d}_0^{(c)}$ are obtained from PFM1 and PFM2 with $\Delta t = 0.02$ sec. Figure 6b shows that PFM2 has the numerical dissipation to eliminate the second mode response since the result obtained from PFM2 is almost overlapped with that obtained from NEM after about 5 sec. Whereas, it is evident that PFM1 leads to an oscillatory response of the second mode for the complete time history since it has no numerical dissipation to damp out the second mode response.

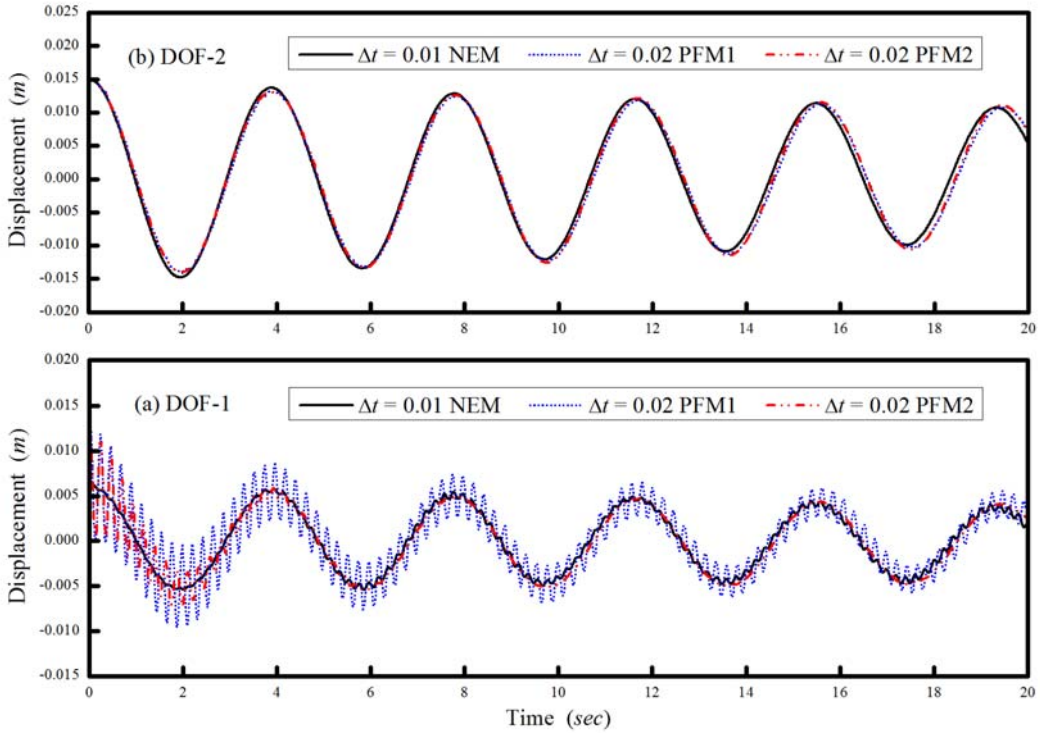

Figure 6 - Free vibration response of 2-degree-of-freedom system

5.2 Seismic Response

Since the pseudodynamic testing method is often used to evaluate the seismic responses of structures, it is of great interest to conduct a series of actual pseudodynamic tests for the 2-degree-of-freedom system subject to an earthquake loading. Notice that the external force vector is no longer zero and an effective earthquake load vector of $\mathbf{p}_{eff} = -\mathbf{M}\ddot{u}_g$ must be added, where $\ddot{u}_g$ is the

ground acceleration. For this purpose, the test setup for the free vibration test is also adopted for the test. The specified mass matrix and the measured initial stiffness matrix are:

$$\mathbf{M} = \begin{bmatrix} 3.0\times10^{4} & 0 \\ 0 & 1.5\times10^{3} \end{bmatrix} kg \qquad \mathbf{K}_{0} = \begin{bmatrix} 7.90\times10^{5} & -1.63\times10^{6} \\ -1.63\times10^{6} & 4.06\times10^{6} \end{bmatrix} N/m\,. \tag{8}$$

As a result, the initial natural frequencies of this system are found to be 2.12 and 52.24 rad/sec. The system is subjected to the 1999 Chi-Chi earthquake record TCU084. The peak ground acceleration of TCU084 is scaled to 0.3g. The pseudodynamic test results are plotted in Fig. 7. The pseudo-dynamic response obtained from NEM with $\Delta t = 0.01$ sec is considered as a reference solution for comparison since the time step is small enough to accurately integrate both modes. On the other hand, a time step of $\Delta t = 0.04$ sec is used for PFM1 and PFM2, where the 1st mode can be very accurately integrated while the 2nd mode will experience significant period distortion. In general, Fig. 7 reveals that both methods can give reliable responses for DOF-2. However, it is interesting to find from Fig. 7a that the test result obtained from PFM1 for DOF-1 is contaminated by the 2nd modal response while PFM2 still provides reliable result. This phenomenon might be explained as follows. It seems that the experimental errors occurred in the 2nd mode are drastically propagated and accumulated and contribute to the total response of DOF-1. However, this error propagation effect can be suppressed by numerical dissipation for using PFM2 and thus it gives a reliable result. Since PFM1 has no numerical damping to suppress the error propagation effect, thus, its result is badly destroyed.

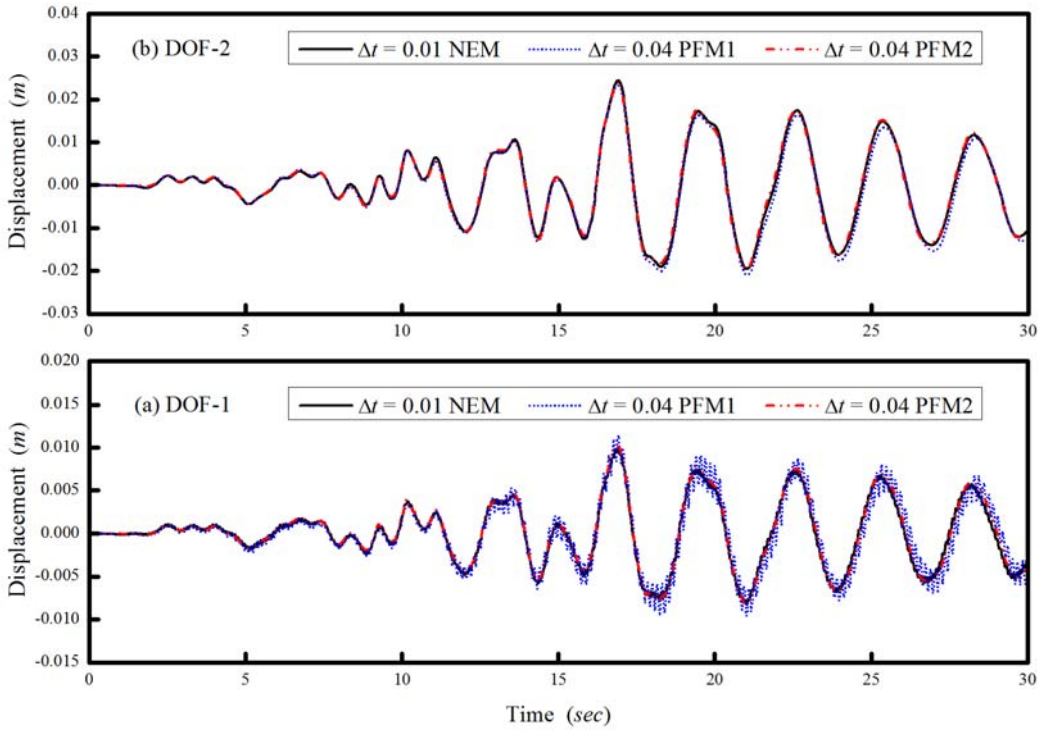

Figure 7 - Seismic response to TCU085 with peak ground acceleration 0.3g

6 CONCLUSION

A new family method is proposed for the pseudodynamic testing. The numerical properties of this family method is very similar to those of HHT–α method. In fact, it can have unconditional stability, second-order accuracy and favourable numerical dissipation, which can be continuously controlled. Hence, both integration methods are very suitable for solving inertial problems, where the low frequency modes can be very accurately integrated while the unimportant high frequency responses can be suppressed or removed by numerical dissipation. Notice that the most important improvement of this family method is that it can have an explicit formulation and thus involves no

nonlinear iterations. Whereas, an iteration procedure is generally needed for HHT $-\alpha$ method. As a result, the pseudodynamic implementation of the proposed family method is much simpler than for HHT $-\alpha$ method. In addition, it is very promising for a substructure test with a large total number of degree of freedom system, where only some selected degrees of freedom are tested, since it is very computationally efficient for conducting the step-by-step integration.

ACKNOWLEDGEMENT

The authors are grateful to acknowledge that this study is financially supported by the National Science Council, Taiwan, R.O.C., under Grant No. NSC-100-2221-E-027-062.

REFERENCES

[1] Takanashi K, Udagawa K, Seki M, Okada T, Tanaka H. Nonlinear earthquake response analysis of structures by a computer-actuator on-line system. Bulletin of Earthquake Resistant Structure Research Center, University of Tokyo, Japan, 1975; 8.

[2] Shing PB, Mahin SA. Cumulative experimental errors in pseudodynamic tests. *Earthquake Engineering and Structural Dynamics* 1987; 15: 409–424.

[3] Shing PB, Mahin SA. Experimental error effects in pseudodynamic testing. *Journal of Engineering Mechanics* (ASCE) 1990; 116: 805–821.

[4] Chang SY. Nonlinear error propagation analysis for explicit pseudodynamic algorithm. *Journal of Engineering Mechanics* (ASCE) 2003; 129 (8): 841–850.

[5] Chang SY. Error propagation in implicit pseudodynamic testing of nonlinear systems. *Journal of Engineering Mechanics* (ASCE) 2005; 131(12): 1257–1269.

[6] Shing PB, Mahin SA. Elimination of spurious higher-mode response in pseudodynamic tests. *Earthquake Engineering and Structural Dynamics* 1987; 15: 425-445.

[7] Chang SY. Improved numerical dissipation for explicit methods in pseudodynamic tests. *Earthquake Engineering and Structural Dynamics* 1997; 26: 917-929.

[8] Nakashima M, Kaminosomo T, Ishida M. Integration techniques for substructure pseudo- dynamic test. *Proceeding of Fourth U.S. National Conference on Earthquake Engineering* 1990; 2:515-524.

[9] Shing PB, Vannan MT, Carter E. Implicit time integration for pseudodynamic tests. *Earthquake Engineering and Structural Dynamics* 1991; 20:551-576.

[10] Thewalt CR, Mahin SA. An unconditionally stable hybrid pseudodynamic algorithm. *Earthquake Engineering and Structural Dynamics* 1995; 24:723-731.

[11] Newmark NM. A method of computation for structural dynamics. *Journal of Engineering Mechanics Division* (ASCE) 1959; 85: 67-94.

[12] Chang SY. Improved numerical dissipation for explicit methods in pseudodynamic tests. *Earthquake Engineering and Structural Dynamics* 1997; 26: 917-929.

[13] Chang SY. Explicit pseudodynamic algorithm with unconditional stability. *Journal of Engineering Mechanics* 2002; 128(9):935–947.

[14] Chang SY. Explicit pseudodynamic algorithm with improved stability properties. *Journal of Engineering Mechanics*, ASCE, 2010; 136(5): 599–612.

[15] Chang SY. An explicit structure-dependent algorithm for pseudodynamic testing. *Engineering Structures*, 2013; 46: 511–525.

[16] Hilber HM, Hughes TJR, Taylor RL. Improved numerical dissipation for time integration algorithms in structural mechanics. *Earthquake Engineering and Structural Dynamics* 1977; 5:283–292.

[17] Chang, SY. A general technique to improve stability property for a structure-dependent integration method," *International Journal of Numerical Methods in Engineering*, Vol. 101, No. 9, pp. 653-669, 2015.

[18] Belytschko T and Hughes TJR. *Computational Methods for Transient Analysis*, 1983, Elsevier Science Publishers B.V., North-Holland.